Tree Physiology 43, 75–87
https://doi.org/10.1093/treephys/tpac110

Research paper

The relative area of vessels in xylem correlates with stem embolism resistance within and between genera

Rodrigo T. Avila[1,2], Cade N. Kane[2], Timothy A. Batz[2], Christophe Trabi[3], Fábio M. Damatta[1], Steven Jansen[3] and Scott A. M. McAdam[2,4]

[1]Departamento de Biologia Vegetal, Universidade Federal de Viçosa, Viçosa, Minas Gerais 36570-900, Brazil; [2]Department of Botany and Plant Pathology, Purdue Center for Plant Biology, Purdue University, West Lafayette, IN 47907, USA; [3]Faculty of Natural Sciences, Institute of Systematic Botany and Ecology, Ulm University, Ulm, Baden-Württemberg 89081, Germany; [4]Corresponding author (smcadam@purdue.edu)

Received May 24, 2022; accepted August 30, 2022; handling Editor Jordi Martinez-Vilalta

The resistance of xylem conduits to embolism is a major factor defining drought tolerance and can set the distributional limits of species across rainfall gradients. Recent work suggests that the proximity of vessels to neighbors increases the vulnerability of a conduit. We therefore investigated whether the relative vessel area of xylem correlates with intra- and inter-generic variation in xylem embolism resistance in species pairs or triplets from the genera *Acer*, *Cinnamomum*, *Ilex*, *Quercus* and *Persea*, adapted to environments differing in aridity. We used the optical vulnerability method to assess embolism resistance in stems and conducted anatomical measurements on the xylem in which embolism resistance was quantified. Vessel lumen fraction (VLF) correlated with xylem embolism resistance across and within genera. A low VLF likely increases the resistance to gas movement between conduits, by diffusion or advection, whereas a high VLF enhances gas transport thorough increased conduit-to-conduit connectivity and reduced distances between conduits and therefore the likelihood of embolism propagation. We suggest that the rate of gas movement due to local pressure differences and xylem network connectivity is a central driver of embolism propagation in angiosperm vessels.

Keywords: drought, gas movement, xylem anatomy.

Introduction

During drought, homoiohydric plants die when the tension on the water column becomes so negative that gas invades the sap-filled xylem, causing widespread embolism and permanently breaking the liquid connection between hydrated photosynthetic tissues and soil water (Sperry and Pockman 1993, Brodribb and Cochard 2009, Cochard and Delzon 2013, Charrier et al. 2016, Lamarque et al. 2018, Brodribb et al. 2021). Plants employ a number of dynamic strategies to avoid reaching these lethal water potentials (Ψ), like closing stomata to reduce water loss (J. Zhang et al. 2016, Choat et al. 2018, Cardoso et al. 2019), plants that construct xylem that is able to resist embolism at more negative Ψ may have a prolonged survival during drought (Cochard et al. 2021).

Many studies have presented correlations between the embolism resistance of xylem conduits and plant tolerance to drought, and have found that embolism resistance can set the distributional limits of species across rainfall gradients (Blackman et al. 2009, Brodribb et al. 2010, Anderegg et al. 2012, Choat et al. 2012, Pittermann et al. 2012, Li et al. 2018). As homogeneous nucleation of a gas bubble in the xylem is physically unlikely at a Ψ less negative than −10 MPa, the behavior of pre-existing bubbles under changing pressure and temperature are likely the primary cause of embolism formation (Hölttä et al. 2002, Kanduč et al. 2020, Ingram et al. 2021). Moreover, gas movement by diffusion or advection (i.e., bulk movement) appears to play a crucial role in this process and is largely determined by gas entry through pit membranes (Sperry and Tyree 1988, Kaack et al. 2019, Zhang et al. 2019, Guan et al. 2021, Avila et al. 2022). Indeed, pit membrane thickness is correlated with embolism resistance across angiosperms (Choat et al. 2008, Li et al. 2016, Kaack et al. 2019, 2021).

The physical and anatomical determinants of air seeding remain poorly understood (Jansen et al. 2018); thus, studies have focused on gross anatomical traits of the xylem to provide additive explanations for variation in embolism resistance across species.

A number of vessel anatomical traits have been associated with differences in P_{50} (or the Ψ at which 50% of the xylem is embolized) between species such as cell wall thickness and vessel diameter ratio $(t/b)^2$ (Hacke et al. 2001, Blackman et al. 2010); vessel diameter (Scoffoni et al. 2016, Venturas et al. 2017); and vessel length (Lens et al. 2011, Jacobsen et al. 2016). Species that have evolved in arid environments and present high resistance to embolism often have high values of $(t/b)^2$ and pit membrane thickness, as well as relatively narrow vessel diameter and short vessel lengths. These adaptive features have likely been selected for because they directly or indirectly impair (i) the initial seeding of embolism events, (ii) the spread of embolism between conduits once an initial embolism has formed or (iii) perhaps even the deformation of vessel conduits under negative pressure.

In addition to the features of individual conduits, recent literature provides compelling evidence that embolism resistance may be determined by gross xylem anatomy, particularly traits that incorporate some metric of the connectivity of vessels (Johnson et al. 2020, Avila et al. 2021, Levionnois et al. 2021, Wason et al. 2021). Inter-vessel connectivity increases hydraulic conductivity but may also increase vulnerability to embolism (Wheeler et al. 2005, Loepfe et al. 2007, Lens et al. 2011, Mrad et al. 2018, 2021, Wason et al. 2021), although the effect of connectivity on embolism resistance may be relatively small due to the multi-layered, safe nature of pit membranes (Kaack et al. 2021, Avila et al. 2022). Connectivity of the vessel network involves various anatomical features, including vessel dimensions (diameter and width), vessel grouping, and the conductive or non-conductive nature of imperforate tracheary elements (i.e., tracheids and fibers). Species with grouped vessels, which are more likely to have non-conductive imperforate tracheary elements (Carlquist 1984, Sano et al. 2011), are more likely to have a relatively low vessel lumen fraction (VLF), and a low vessel density for a given vessel diameter (Martínez-Vilalta et al. 2012). As such, VLF represents the product of the mean vessel diameter and vessel density, and can be considered as an indirect measure of connectivity (Zanne et al. 2010). Connectivity between vessels is rather poorly understood due to practical difficulties with 3D vessel network reconstructions (Zimmermann and Tomlinson 1966, Brodersen et al. 2011), whereas it is also unknown how exactly vessel connectivity relates to vessel dimensions and the presence/absence of tracheids. Moreover, it is unclear how these connectivity characters relate directly or indirectly to embolism propagation, which is known to occur from an embolized to a sap-filled vessel (Brodersen et al. 2013, Choat et al. 2016, Guan et al. 2021, Pritzkow et al. 2022). For this reason, we hypothesize that VLF is related to embolism resistance because a higher conduit fraction facilitates gas movement, which has been suggested to increase the likelihood of embolism formation (Guan et al. 2021, Avila et al. 2022).

To test this hypothesis, we made comparisons of xylem anatomy and embolism resistance in species pairs or triplets, native to regions of differing aridity, in five genera. Some of the best examples of the adaptive relevance of embolism resistance to plant survival in dry environments are provided by studies that have examined the variation in embolism resistance across genera with a wide distributional range. In 23 species of *Callitris* from across the range of the genus, a variation in mean species-specific P_{50} is driven by aridity gradients across the continent of Australia (Larter et al. 2017). Considerable variability in embolism resistance across species has also been reported in the genus *Quercus* with species-specific P_{50} ranging from −2.72 to −6.27 MPa across the genus (Skelton et al. 2018). This variation in *Quercus* is correlated with the aridity of native ranges (Skelton et al. 2021). Across species in the genus *Acer* P_{50} also correlates with habitat preferences (Lens et al. 2013, Schumann et al. 2019). *Acer campestre*, a species that occurs commonly in more arid areas of Europe and Asia Minor, has a P_{50} of −5.40 MPa, whereas the more mesic adapted species *Acer pseudoplatanus* has a P_{50} of −3.10 MPa (Schumann et al. 2019).

Here, we investigate whether species with more vulnerable xylem have xylem anatomy and network traits more conducive to embolism propagation between conduits, including higher VLF. We examine embolism resistance and xylem anatomy across 11 species from 5 genera, which evolved in contrasting environments varying in aridity, to investigate whether gross xylem anatomical drivers correlate with intrageneric variation in embolism resistance, namely vessel characteristics including vessel diameter, wall thickness and VLF. We used the optical vulnerability method for detecting embolism in stem xylem to construct vulnerability curves (Brodribb et al. 2016) and also conducted an experiment to test the validity of this non-hydraulic method by the simultaneous measurement of stem vulnerability curves in two species of *Acer* with the Chinatron centrifuge (Wang et al. 2014).

Materials and methods

Plant material

To assess intrageneric variation in embolism resistance and xylem anatomy, we selected species from the genera *Acer* (Sapindaceae), *Cinnamomum* (Lauraceae), *Ilex* (Aquifoliaceae), *Quercus* (Fagaceae) and *Persea* (Lauraceae), which evolved in contrasting environments (Table S1 available as Supplementary data at *Tree Physiology* Online). Plants of *Acer pseudoplatanus* L. and *A. campestre* L. were wild-grown trees in the grounds of

the Botanical Garden of Ulm University, Ulm (Germany) (48° 25′ N, 9° 57′ E), *Ilex paraguariensis* A.St.-Hill was ~20 years old and a 4-m-tall shrub grown in the glasshouses of the Botanical Gardens of Ulm University, and *Cinnamomum cassia* (L.) J.Presl, *C. camphora* (L.) J.Presl, *Persea americana* Mill., *P. indica* (L.) Spreng, *Quercus falcata* Michx., *Q. robur* L., *Q. rubra* L. and *Ilex verticillata* (L.) A.Gray were 3-year-old seedlings grown in the glasshouses of Purdue University, West Lafayette (Indiana, USA) (40° 25′ N, 86° 54′ W, elevation: 187 m). Samples of *I. verticillata* were also taken from three mature shrubs grown outside on the grounds of Purdue University. Experiments performed in West Lafayette and Ulm were conducted between August and early October 2018 and June and July 2019, respectively.

Vulnerability curves

Measurements of vulnerability curves in stems were conducted using the optical vulnerability method (Brodribb et al. 2016) with stereo microscopes (SZMT2, optika, Italy) and Raspberry Pi clamps (opensourceOV.org). ChinaTron (Model H2100R, Xiangui, China) centrifuge vulnerability curves were also obtained using 27.4-cm-long stem segments of the two *Acer* species taken from the same three plants used to assess vulnerability with the optical method, as these species have relatively short vessels (Schumann et al. 2019). Three 2-m-long branches, collected before dawn in July 2019, were used to construct centrifuge vulnerability curves as described by Guan et al. (2022). Samples were not flushed prior to assessing vulnerability, as flushing was not performed on the paired branches for which the optical vulnerability method was used. A reference solution of 10-mM KCl was used.

For optical vulnerability curves, three stems of each species (each stem from a different individual) were cut under water early in the morning (0.6–2.5 m long, depending on the species) and placed inside a closed bag containing moist paper towels for 1 h to equilibrate water potential. A small, terminal stem of current year growth only was selected for analysis between 0.35 and 2.2 m from the open cut to avoid open vessel artifacts. These terminal stems had a diameter of 7–11 mm and were randomly selected on the harvested branch. A location along this branch 0.3 m from apex was selected to avoid the strongest effects of developmentally driven vessel tapering (Petit et al. 2008, Olson et al. 2014) and the bark was gently removed by hand, with care taken to not touch the xylem. Immediately after bark removal, an adhesive gel (Tensive) was spread onto the exposed xylem and a coverslip placed over the gel. This region was enclosed in the imaging clamp or placed under a stereo microscope. Branches were allowed to dry in darkness while images were taken every 3 min and Ψ assessed every 10 min using a PSY1 stem Psychrometer (ICT International, version 4.4) that was installed at least 0.2 m from the imaged area. In *I. verticillata*, Ψ until leaf death was concurrently measured in small branches bearing up to five leaves using a Scholander Pressure Chamber (PMS Instrument Company, Model 1505D).

Stem anatomy

Stem xylem anatomy was observed in a central segment of the area of the stem that was directly imaged to generate optical vulnerability curves. For the centrifuge curves, a sample was taken from the middle of the stem segment that was used to construct curves. Transverse sections (25-μm thick) were made using a freezing stage-microtome (Thermo scientific, model: HM 430) stained with aqueous 5% toluidine blue and mounted in phenol glycerine jelly. To determine vessel diameter, $(t/b)^2$, and VLF, images were taken with an Axiocam 506 color camera connected to a light microscope (Zeiss Axio Imager.A2 at 10× and 5× magnification and amplified by a 1.6× magnification tube). All anatomical traits were measured using ImageJ software on the newest season growth rings and all data were collected before the formation of latewood in the ring-porous *Quercus* species, but after leaf flushing.

Double wall thickness (t) and corresponding vessel lumen diameter (b) was determined in 125 vessels from stems for each sample. The cell wall thickness was measured between two xylem vessels (avoiding cell wall corners) and the lumen diameter was calculated from the vessel area. Assuming that vessel lumen in cross-section was an approximate circle, the diameter was estimated using Eq. (1), where b is the vessel lumen diameter and A is the area of the vessel lumen:

$$b = 2 \times \sqrt{A/\pi}. \quad (1)$$

Vessel lumen fraction was determined by summing all A values for each cross-section and expressing this area as a percentage of total xylem area using Eq. (2). For stems, the VLF values were based on wood tissue, whereas the VLF measurements of leaves were based on xylem of the vascular bundle.

$$\text{VLF} = \frac{\sum A}{\text{Xylem area}} \times 100. \quad (2)$$

Data analysis

Mean optical vulnerability curve data for each species were generated by calculating the mean and standard error Ψ measured at each 1% increment of the embolized xylem area from the three curves constructed. This approach constructs a mean scaled empirical cumulative distribution of embolism for each species, a method that provides a more accurate estimate of P_{50}, and other cardinal water potentials, than sigmoidal or exponential model fitting to optical vulnerability datasets (Cardoso et al. 2022). Mean P_{50} for each species was used to test for significant linear correlations with key anatomical

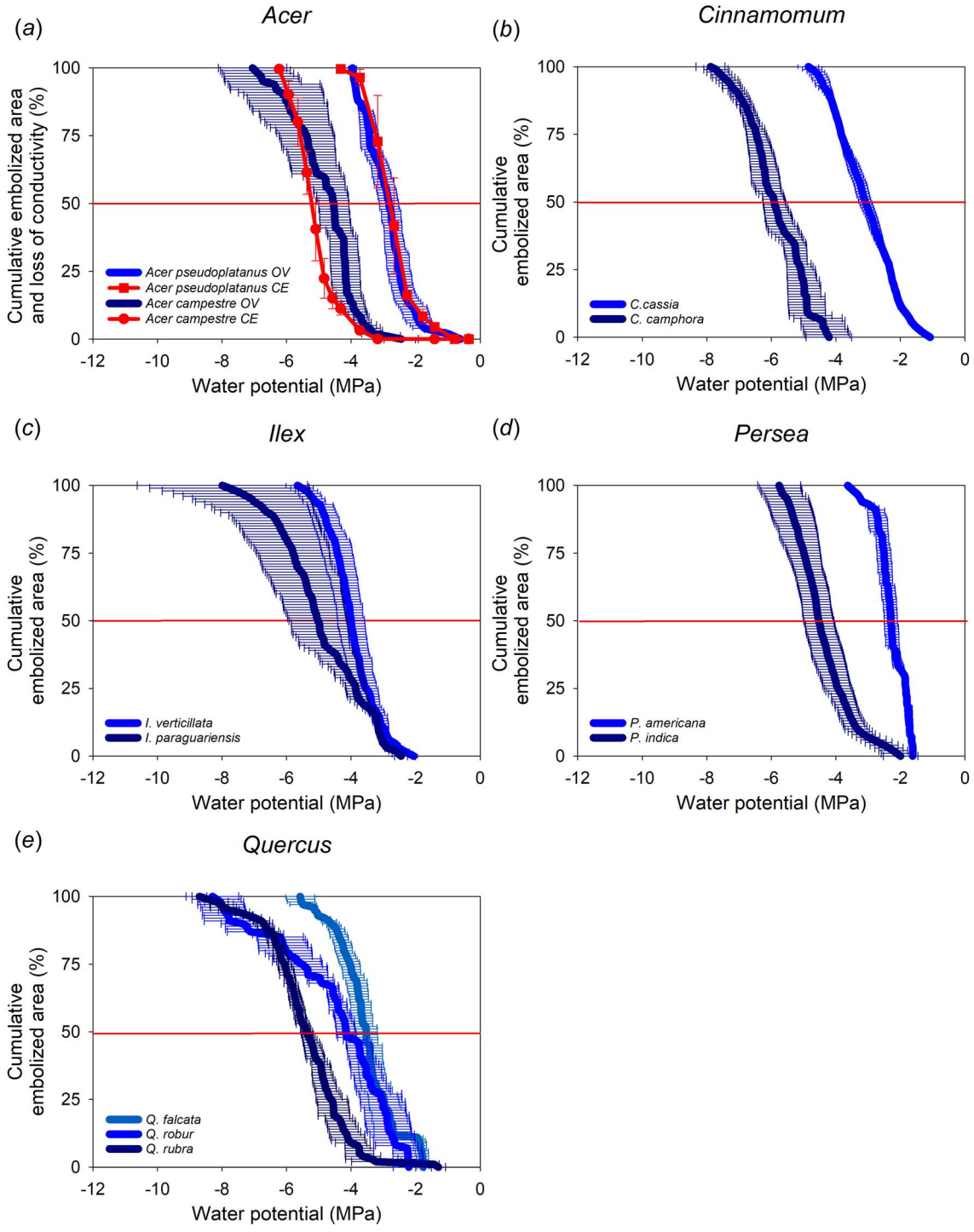

Figure 1. Optical (blue, OV) and centrifuge (red, CE) vulnerability curves of stems in angiosperm species (each represented by curves of a different shade (OV), or symbol (CE) in *Acer* (a), *Cinnamomum* (b), *Ilex* (c), *Persea* (d) and *Quercus* (e) ($n = 3$, error bars represent ±SE)). See Table 1 for mean P_{50} values for each species.

traits by fitting linear regressions using SigmaPlot v.10 software (Systat Software, Germany). Tests for differences in embolism resistance and anatomical traits within and between genera were performed using ANOVAs with post hoc Tukey's test using R software (version 4.1.2).

Results

A large intrageneric variation in stem P_{50}

We found a large variation in stem P_{50} ranging from −2.07 up to −6.80 MPa across all species measured (Figure 1, Table 1). Between species in the same genus, we found significant

Table 1. Mean stem water potential at which 50% of the stem xylem area was embolized (P_{50}) and standard error ($n = 3$), in addition to mean vessel diameter and inter-vessel wall thickness ($n = 125$) for each species examined. P_{50} values were based on the optical method, except for the two *Acer* species studied, which also included flow-centrifuge measurements. Different letters denote a significant difference in species within each genus ($P < 0.05$).

Species	Method	P_{50} (MPa)	SE	VLF (%)	SE	Vessel diameter (μm)	SE	Inter-vessel wall thickness (μm)	SE
Acer pseudoplatanus	Optical	−2.87a	0.24	13.71	0.23	26.95	1.3	2.99	0.18
	Centrifuge	−2.83a	0.3	14.59	0.52	28.08	3.1	3.29	0.09
Acer campestre	Optical	−5.2b	0.12	10.66	0.86	25.33	0.87	2.64	0.11
	Centrifuge	−4.55b	0.5	9.34	0.71	30.04	1.8	2.8	0.1
Cinnamomum cassia	Optical	−3.08a	0.2	8.93	0.46	35.79	2.38	3.83	0.12
Cinnamomum camphora	Optical	−5.9b	0.35	5.86	0.77	30.63	1.33	3.28	0.12
Ilex verticillata	Optical	−4	0.42	16.58	2.35	25.51	1.32	3.96	0.16
Ilex paraguariensis	Optical	−5.03	0.89	9.58	2.14	19.07	3.24	4.45	0.21
Persea americana	Optical	−2.3a	0.2	12.98a	2.13	27.31	0.22	2.98a	0.04
Persea indica	Optical	−4.53b	0.47	4.66b	0.49	32.49	1.4	3.94b	0.01
Quercus falcata	Optical	−3.53a	0.35	16.81	1.49	41.46	5.86	3.18	0.11
Quercus robur	Optical	−4ab	0.42	12.02	2.74	35.53	4.26	3.16	0.12
Quercus rubra	Optical	−5.03b	0.89	11.35	1.15	40.29	6.69	3.71	0.28

differences in mean embolism resistance (ANOVA, $F(12, 26) = 8.023$, $P < 0.001$), with the exception of *Ilex*, in which the Northern Hemisphere temperate deciduous species *I. vercitillata* and the Southern Hemisphere subtropical evergreen species *I. paraguariensis* had a similar mean (±SE) P_{50} (−4.00 ± 0.42 MPa and − 5.03 ± 0.89 MPa, respectively) (Figure 1). *Persea americana*, native to subtropical rainforest, was more vulnerable than the Macronesian native *P. indica*, (P_{50} −2.30 ± 0.20 MPa, compared with −4.53 ± 0.47 MPa, respectively). *Cinnamomum cassia*, which is native to mildly seasonal subtropical forests, had a mean (±SE) stem P_{50} of −3.08 ± −0.20 MPa, which was more vulnerable than the stems of *C. camphora*, native to highly seasonal subtropical forests with a mean (±SE) stem P_{50} of −5.90 ± 0.35 MPa. A modest variation in mean stem P_{50} was observed across *Quercus* species with *Q. falcata*, *Q. robur* and *Q. rubra* having a mean (±SE) stem P_{50} of −3.53 ± 0.35, −4.00 ± 0.42 and − 5.03 ± 0.89 MPa, respectively. In *Acer*, the optical method and the Chinatron centrifuge were used to construct vulnerability curves. Post hoc Tukey's test revealed no significant difference between the mean (±SE) P_{50} generated by either method in *Acer*, with means from both methods being −2.87 ± 0.24 and −5.2 ± 0.12 MPa, respectively, for *A. pseudoplatanus* and *A. campestre* (Figure 1a, Table 1).

Anatomical features correlated with P_{50}

We found considerable variation in VLF between species of the same genus, ranging from between 11 and 16% across species of *Quercus* and between 4 and 12% in the two species of *Persea* (Figure 2). This difference in VLF was visibly apparent in transverse sections, particularly between the two *Persea* species (Figure 3). Across all genera, the higher the VLF, the more vulnerable the stem xylem was to embolism. Mean stem P_{50} correlated with VLF within each of the five genera examined, as well as across all samples pooled together (linear regression, $t(37) = 3.7629$, $P < 0.001$, r = 0.53) (Figure 2).

There was considerable variation in the vessel diameter (ANOVA, $F(12, 26) = 4.24$, $P < 0.001$) and wall thickness (ANOVA, $F(12, 26) = 8.02$, $P < 0.001$) across the species sampled (Table 1, Figures 4 and 5). Mean vessel diameter ranged from 19 ± 3.24 μm in *I. paraguariensis* to 41.5 ± 5.9 μm in *Q. falcata* (Table 1). Species pairs in the genera *Acer*, *Persea* and *Quercus* had similar mean vessel diameters (Table 1). Neither the vessel diameter (Figure 4) nor wall thickness (Figure 5) correlated with P_{50} across all species. A post hoc Tukey's test showed that there was a significant difference ($P < 0.01$) in the mean vessel diameter between the two species of *Cinnamomum*, with *C. camphora*, which had a more negative P_{50} than *C. cassia*, having the narrowest vessels (30.6 ± 1.3 to 35.8 ± 2.4 μm, respectively) (Figure 4, Table 1). This was the only species pair to display a significant positive relationship between the vessel diameter and P_{50} (Figure 4c; linear regression, $t(5) = 2.78$; $P < 0.05$, $r = 0.81$). By contrast, we observed a significant negative linear correlation between vessel diameter and P_{50} in the two species of *Persea* (Figure 4e; linear regression, $t(5) = -7.22$, $P < 0.01$, $r = 0.96$).

Inter-vessel wall thickness varied across the species sampled with the narrowest wall thickness observed in *A. campestre* (2.64 ± 0.11 μm), whereas the thickest inter-vessel wall thickness was observed in *I. paraguariensis* (4.45 ± 0.21 μm) (Table 1). Mean inter-vessel wall thickness did not vary across

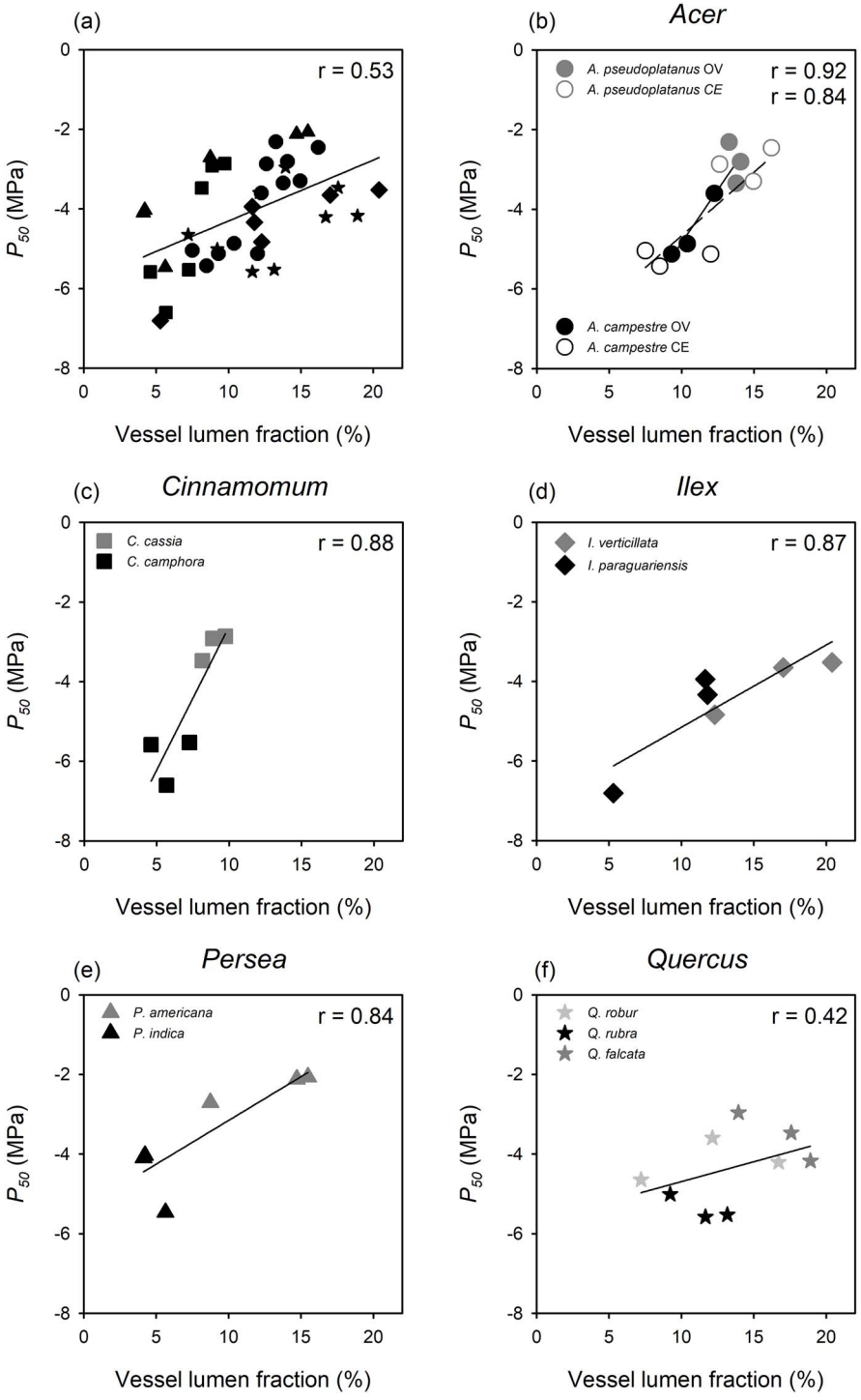

Figure 2. The relationship between vessel lumen fraction (VLF) and water potential at which 50% of xylem area was embolized or 50% of conductivity was lost (P_{50}) in *Acer* (circles), *Cinnamomum* (squares), *Ilex* (diamonds), *Persea* (triangles) and *Quercus* (stars) (a). The relationships between VLF and P_{50} in each genus including *Acer* (b), for this genus data from both optical (OV—closed symbols) and centrifuge sampled stems (CE—open symbols) are shown, *Cinnamomum* (c), *Ilex* (d), *Persea* (e) and *Quercus* (f). Species within each genus in panels (b)–(f) are represented by symbols of a different shade, significant linear regressions are shown.

species from the genera *Acer*, *Ilex* and *Quercus* (Table 1). In the genus *Cinnamomum*, we observed a significant positive linear correlation between inter-vessel wall thickness and P_{50} (linear regression, $t(5) = 3.99$, $P < 0.05$, $r = 0.89$), with the samples that had more vulnerable xylem having the thinnest walls (Figure 5c). By contrast, the only other genus in which we saw a relationship between wall thickness and embolism resistance was *Persea*, in which we observed a significant

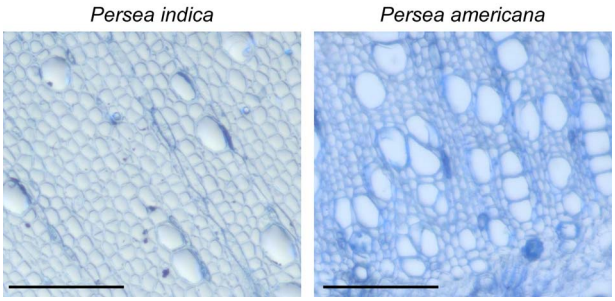

Figure 3. Transverse section through the stem xylem of *P. indica* and *P. americana*. Scale bars = 100 μm.

negative linear relationship between vessel wall thickness and P_{50} (linear regression, $t(5) = -4.19$, $P < 0.05$, $r = 0.9$), with the most embolism resistant samples having the thickest walls (Figure 5e).

Discussion

We found that VLF correlated with P_{50} across 11 species from five genera. A lower VLF was observed in species adapted to more arid or seasonal environments than in closely related species in the same genus native to more mesic environments. Similar correlations between VLF and mean annual rainfall have been observed across 51 species native to California (Preston et al. 2006). This environmental and functional link with VLF also manifests in correlations with wood density and theoretical conductivity (Zanne et al. 2010).

Given the emergent nature of VLF, being a function of numerous anatomical traits linked to embolism resistance including the vessel connectivity, vessel size, density and potentially wall thickness, it seems most likely that the correlations we find here are due to the indirect nature of the trait on embolism resistance. There is ample evidence that embolism spreads from an embolized conduit to an adjacent, sap-filled conduit, with embolism formation in isolated conduits not connected to any neighboring embolized conduits being rare (Brodersen et al. 2013, Brodribb et al. 2016, Choat et al. 2016, Guan et al. 2021, Wason et al. 2021, Avila et al. 2022). When a conduit becomes embolized, it is initially filled with 100% water vapor (0.003 MPa at 25 °C), but will undergo a gradual build-up of bubble pressure to atmospheric pressure, with gas diffusion over different spatial scales (Wang et al. 2014). This pressurization process represents a buffering process to further embolism spread and may take several hours to days, depending on the gas diffusion kinetics across cell walls and pit membranes (Sorz and Hietz 2006, Wang et al. 2014). Given that isolated embolism events are rare, we would assume that gas movement (including both dissolved and undissolved gas) plays a major role in embolism propagation, especially along the resulting pressure differential between an embolized and sap-filled conduit (Jansen et al. 2020, Guan et al. 2021). There is evidence that individual conduits in the xylem have specific Ψ thresholds at which embolism will form, but that once a substantial proportion of gas has entered the xylem tissue, embolism will rapidly propagate through the remaining hydrated xylem (Avila et al. 2022). We suggest that when VLF is low, due to one or more key wood anatomical traits related to the connectivity or distance between conduits being altered, the spread of embolism between conduits is reduced. Our work here further emphasizes that more investigation is required to understand the importance of the 3D vessel network in future studies on embolism resistance (Loepfe et al. 2007, Wason et al. 2021).

Bordered pits will only develop in a conduit wall that is connected to another vessel or a tracheid, whereas pits do not occur between a vessel and non-conductive imperforate tracheary elements (Sano et al. 2008, 2011). In this way, fibers that are gas-filled and not holding any capillary water are unlikely to provide gas sources for fast embolism spread in neighboring conduits, as the gas movement across the wall should be much slower than across thin, mesoporous pit membranes. Also, xylem tissue that does not embolize (Y. Zhang et al. 2016) and contributes very little to water transport, including living fibers and parenchyma, may impair the spread of gas through the xylem (Jacobsen et al. 2005). This avoidance of embolism spread by the non-conduit xylem matrix may translate to changes in xylem vulnerability, with more negative Ψ required to trigger embolism formation in more protected vessels (Loepfe et al. 2007, Johnson et al. 2020, Avila et al. 2021, Levionnois et al. 2021, Wason et al. 2021). By contrast, when vessels are packed into xylem in close proximity, with a minimal non-vessel matrix, gas movement between vessels would be relatively fast, and the chance of embolism spreading between adjacent vessels at negative Ψ increases, increasing the vulnerability of the xylem. Species with greater lignification have more embolism-resistant xylem due to increased lignification of conduits, a high amount of imperforate tracheary elements, such as fibers in the ground tissue of the xylem, or sclerenchyma surrounding vascular bundles (Lens et al. 2016, Dória et al. 2018). The lignin composition, in particular the ratio of guaiacyl to syringyl, may also be related to embolism resistance (Lima et al. 2018, Pereira et al. 2018).

We find that vessel conduit dimensions, especially diameter and wall thickness (Figures 4 and 5), are not good sole predictors of embolism resistance, and there is currently no direct, mechanistic explanation for a putative vessel diameter–P_{50} relationship. More detailed analyses, however, would be needed to test this relationship between vessel diameter and P_{50} at the inter- and intra-generic level. This contrasts with numerous earlier studies that find correlations in cell wall thickness and vessel diameter ratio $(t/b)^2$ (Hacke et al. 2001, Blackman et al. 2010), the diameter of vessels (Scoffoni et al. 2016,

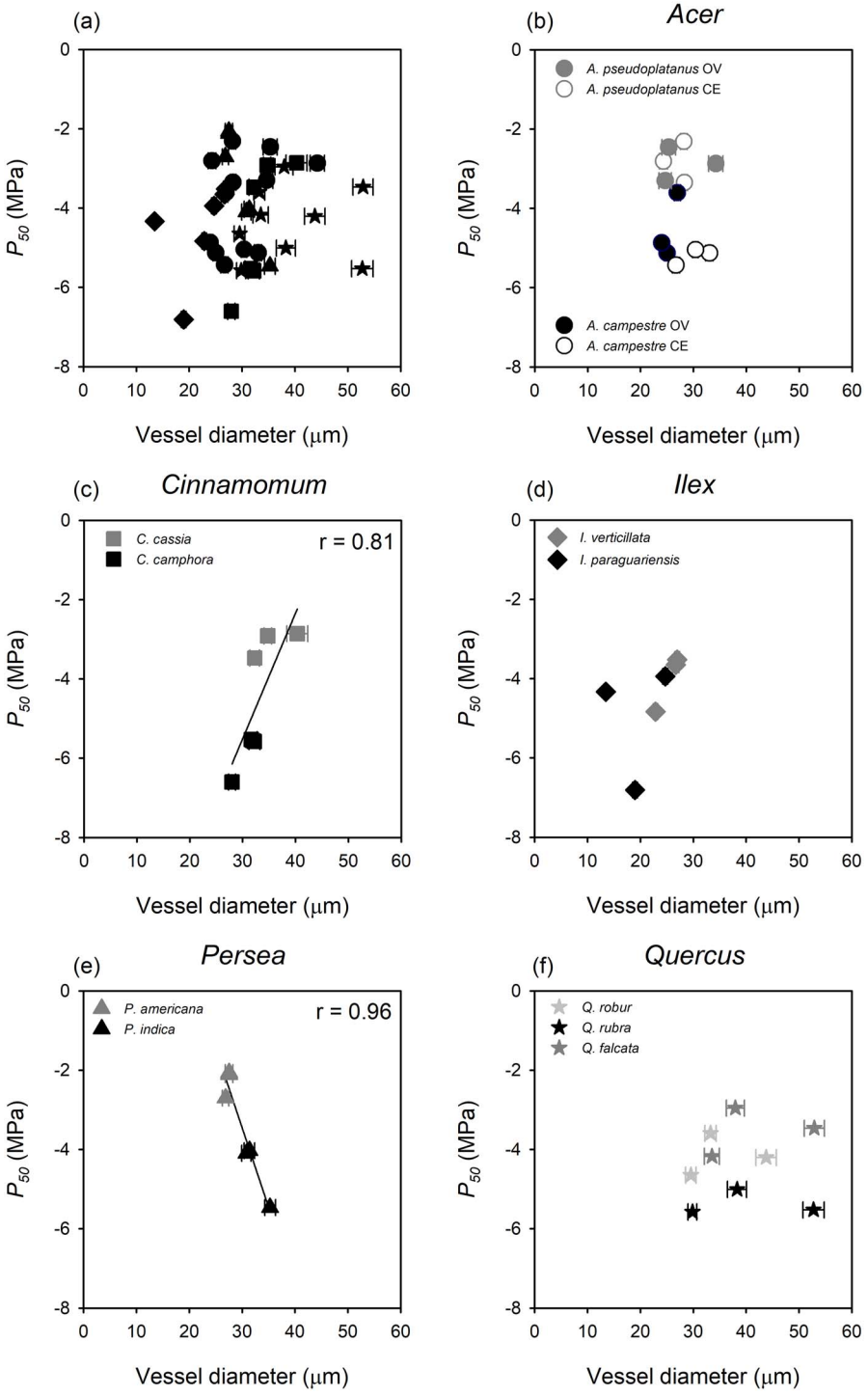

Figure 4. The relationship between mean vessel diameter (±SE) and water potential at which 50% of xylem area was embolized or 50% of conductivity was lost (P_{50}) in *Acer* (circles), *Cinnamomum* (squares), *Ilex* (diamonds), *Persea* (triangles) and *Quercus* (stars) (a). The relationships between vessel diameter and P_{50} in each genus including *Acer* (b), for this genus data from both optical (OV—closed symbols) and centrifuge sampled stems (CE—open symbols) are shown, *Cinnamomum* (c), *Ilex* (d), *Persea* (e) and *Quercus* (f). Species within each genus in panels (b)–(f) are represented by symbols of a different shade, significant linear regressions are shown.

Hacke et al. 2017) and vessel length (Lens et al. 2011, Jacobsen et al. 2016) with inter-specific variation in xylem vulnerability. Our results suggest that these observations may not be universal. Indeed, within a species, vessel diameter is largely driven by size-related trends that could complicate relationships between this trait and P_{50}. Interestingly, the thickness and chemistry of secondary walls in leaf mesophyll was found to be an important determinant of CO_2 diffusion and

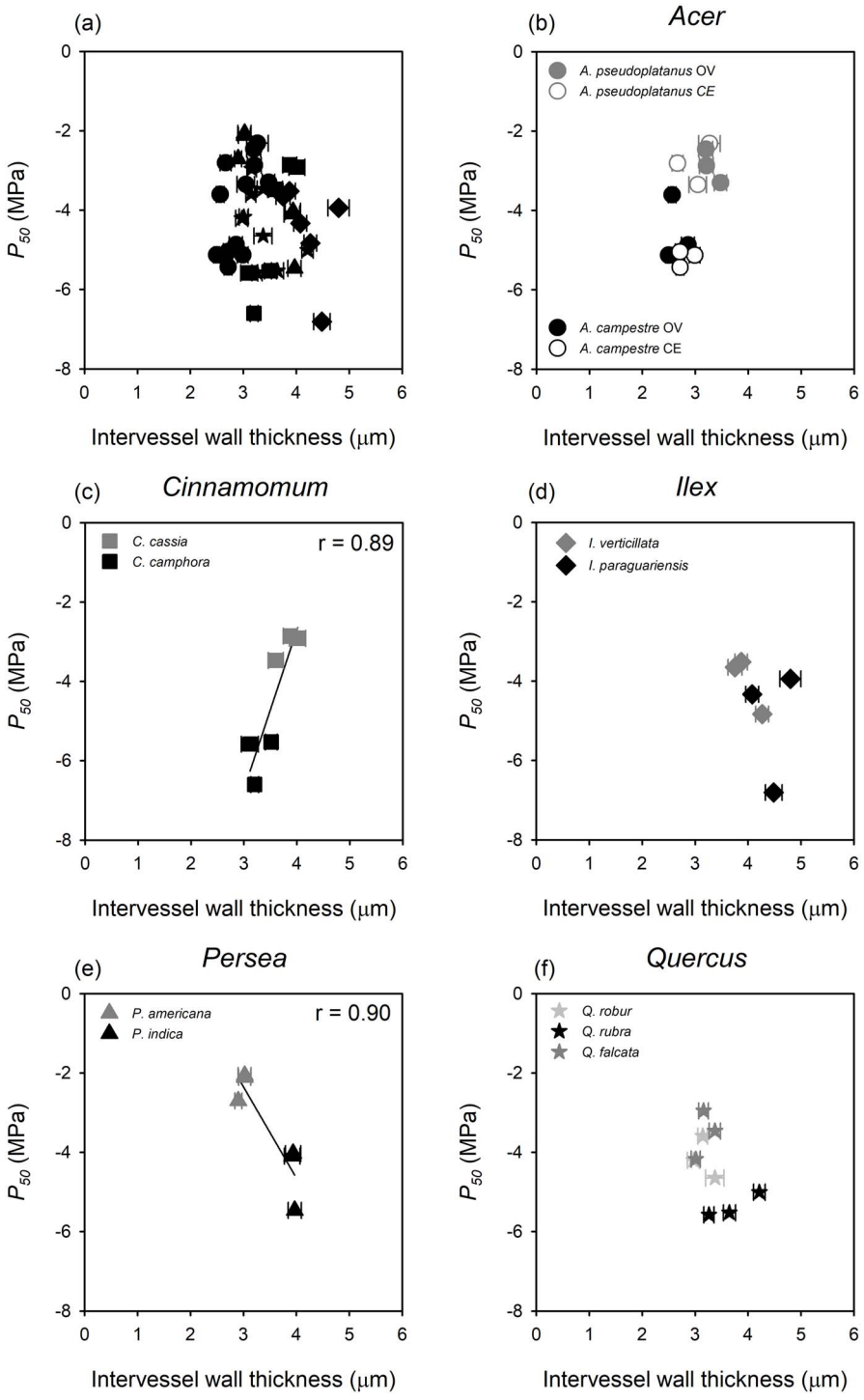

Figure 5. The relationship between mean inter-vessel wall thickness (±SE) and water potential at which 50% of the xylem area was embolized or 50% of conductivity was lost (P_{50}) in *Acer* (circles), *Cinnamomum* (squares), *Ilex* (diamonds), *Persea* (triangles) and *Quercus* (stars) (a). The relationships between inter-vessel wall thickness and P_{50} in each genus including *Acer* (b), for this genus data from both optical (OV—closed symbols) and centrifuge sampled stems (CE—open symbols) are shown, *Cinnamomum* (c), *Ilex* (d), *Persea* (e) and *Quercus* (f). Species within each genus in panels (b)–(f) are represented by symbols of a different shade, significant linear regressions are shown.

photosynthetic efficiency (Flexas et al. 2021, Roig-Oliver et al. 2021). However, wall thickness of vessels does not seem to affect embolism spread, most likely because pit membranes in bordered pit pairs are estimated to provide ca. 100 times less resistance to gas flow than cell walls (Yang et al. 2022). How alterations in VLF are driven by variation in vessel-to-vessel connectivity, vessel and imperforate tracheary connections, and understanding the importance of these connections in preventing embolism spread could be useful for a deeper understanding about the drivers of embolism resistance, and

should be a matter for future studies (Choat et al. 2005, 2016, Rockwell et al. 2014, Charrier et al. 2016, Hochberg et al. 2016, 2017).

We observed a considerable variation in embolism resistance between species from five genera, with consistent observations of species adapted to more arid environments having lower mean P_{50}. Studies investigating variation in embolism resistance across species from the same genus are relatively common, and a similar variation is often detected (Choat et al. 2012, Lobo et al. 2018, Skelton et al. 2021), suggesting that the evolution of resistant xylem is evolutionarily dynamic and highly adaptive at the species level. For many of the species in this study, this is the first report of stem embolism resistance to our knowledge. In some species, there are reports of embolism resistance determined by various methods, some of which are prone to long-vessel artifacts. There are two reports of stem P_{50} in *C. camphora* being −1.24 (Vander Willigen et al. 2000) and −3 MPa (Kröber et al. 2014). Both studies used the high-pressure flow meter on short stem segments, which might explain why the P_{50} we report here for this species using the optical method was much lower at −5.9 MPa (Table 1). In *Quercus*, there have been many studies in which embolism resistance has been determined using approaches prone to long-vessel artifacts (Tyree and Cochard 1996, Maherali et al. 2006). More recently, there have been reports of P_{50} values in species from this genus using branches that exceed the length of the longest vessel (Lobo et al. 2018, Skelton et al. 2021). Lobo et al. (2018) measured embolism resistance in mature, field grown trees in Europe of *Q. rubra* and *Q. robur* and found mean P_{50} values of -4.43 ± 0.25 and -4.74 ± 0.09 MPa, respectively. There was no or only minor significant differences between the P_{50} values measured in this study in greenhouse grown saplings and those measured in mature field grown trees (-5.03 ± 0.89 and -4 ± 0.42 MPa for *Q. rubra* and *Q. robur*, respectively (*t*-tests, $P = 0.42$ in *Q. rubra* and $P = 0.021$ in *Q. robur*). The two species of *Acer* in this study were selected because they have relatively short vessels allowing for accurate measurements of embolism resistance using a centrifuge, and our results here are similar to previously published data for these two species (Rosner et al. 2019, Schumann et al. 2019). Schumann et al. (2019) have suggested that the increased embolism resistance of *A. campestre* compared with two other widespread native European *Acer* species is due to adaptation to drier microsites.

In this study, we conducted a comparison between the vulnerability curves generated by the optical vulnerability technique and the hydraulic curves generated by the Chinatron centrifuge. We found that both methods produced similar vulnerability curves in the two species of *Acer* in which this experiment was conducted, with both methods yielding similar estimates of P_{50} (Figure 1). This result adds to a body of literature demonstrating close agreement in stem vulnerability curves constructed by the optical vulnerability technique and hydraulic methods (Brodribb et al. 2017, Skelton and Diaz 2020), pneumatic method (Guan et al. 2021) and microCT (Pratt et al. 2019, Gauthey et al. 2020, Johnson et al. 2020). A recent study by Venturas et al. (2019), which found no relationship between a curve generated by the optical method and both hydraulic or microCT methods, used an unconventional approach to estimating embolism resistance from optical data, arbitrarily assigning each embolism event, regardless of size, a similar weight. We would not recommend this approach in future studies, but would instead recommend quantifying embolism area and presenting vulnerability curves in terms of the percentage accumulated embolized area.

Conclusions

In conclusion, we found that VLF correlates with stem xylem resistance consistently across species. This correlation was found across clades of species adapted to different aridities, which might be due to the emergent nature of this key xylem anatomical trait, incorporating a suite of vessel and xylem traits associated with embolism resistance. In this way, P_{50} may not just be a function of how resistant an individual xylem conduit is, but also a function of how easily incipient embolism might spread through the conduit network in xylem.

Authors' contributions

R.T.A. collected and analyzed optical vulnerability curves and prepared samples for and quantified xylem anatomy traits, helped design the study and drafted the manuscript; C.N.K. assisted with optical vulnerability curves and sample preparation for anatomy; T.A.B. assisted with optical vulnerability curves; S.J. and F.M.D. critically revised the manuscript and helped with the study design; S.J. and C.T. performed the centrifuge vulnerability curves; S.A.M.M. conceived and designed the study, assisted with all data collection and helped draft the manuscript with S.J. S.A.M.M. and F.M.D. supervised the project. S.A.M.M. and R.T.A. conceived the original ideas.

Supplementary data

Supplementary data for this article are available at *Tree Physiology* Online.

Acknowledgments

We thank two reviewers, the editor, as well as Tim Brodribb and Jarmila Pittermann for helpful comments.

Funding

This work was supported by the USDA National Institute of Food and Agriculture (Hatch project 1014908) and an Alexander von Humboldt Fellowship to S.A.M.M.; CNPq-CAPES (R.T.A.); and a research grant from the German Research Foundation (DFG,

Deutsche Forschungsgemeinschaft, Project nr 457287575) to S.J.

Conflict of interest

None declared.

References

Anderegg WRL, Berry JA, Smith DD, Sperry JS, Anderegg LDL, Field CB (2012) The roles of hydraulic and carbon stress in a widespread climate-induced forest die-off. Proc Natl Acad Sci USA 109:233–237.

Avila RT, Cardoso AA, Batz TA, Kane CN, DaMatta FM, McAdam SAM (2021) Limited plasticity in embolism resistance in response to light in leaves and stems in species with considerable vulnerability segmentation. Physiol Plant 172:2142–2152.

Avila RT, Guan X, Kane CN, Cardoso AA, Batz TA, DaMatta FM, Jansen S, McAdam SAM (2022) Xylem embolism spread is largely prevented by interconduit pit membranes until the majority of conduits are gas-filled. Plant Cell Environ 45:1204–1215.

Blackman CJ, Brodribb TJ, Jordan GJ (2009) Leaf hydraulics and drought stress: response, recovery and survivorship in four woody temperate plant species. Plant Cell Environ 32:1584–1595.

Blackman CJ, Brodribb TJ, Jordan GJ (2010) Leaf hydraulic vulnerability is related to conduit dimensions and drought resistance across a diverse range of woody angiosperms. New Phytol 188:1113–1123.

Brodersen CR, Lee EF, Choat B, Jansen S, Phillips RJ, Shackel KA, McElrone AJ, Matthews MA (2011) Automated analysis of three-dimensional xylem networks using high-resolution computed tomography. New Phytol 191:1168–1179.

Brodersen CR, McElrone AJ, Choat B, Lee EF, Shackel KA, Matthews MA (2013) In vivo visualizations of drought-induced embolism spread in *Vitis vinifera*. Plant Physiol 161:1820–1829.

Brodribb T, Brodersen CR, Carriqui M, Tonet V, Rodriguez Dominguez C, McAdam S (2021) Linking xylem network failure with leaf tissue death. New Phytol 232:68–79.

Brodribb TJ, Cochard H (2009) Hydraulic failure defines the recovery and point of death in water-stressed conifers. Plant Physiol 149:575–584.

Brodribb TJ, Bowman DJMS, Nichols S, Delzon S, Burlett R (2010) Xylem function and growth rate interact to determine recovery rates after exposure to extreme water deficit. New Phytol 188:533–542.

Brodribb TJ, Skelton RP, Mcadam SAM, Lucani CJ, Marmottant P (2016) Visual quantification of embolism reveals leaf vulnerability to hydraulic failure. New Phytol 209:1402–1409.

Brodribb TJ, Carriqui M, Delzon S, Lucani C (2017) Optical measurement of stem xylem vulnerability. Plant Physiol 174:2054–2061.

Cardoso AA, Randall JM, McAdam SAM (2019) Hydraulics regulate stomatal responses to changes in leaf water status in the fern *Athyrium filix – femina*. Plant Physiol 179:533–543.

Cardoso AA, Kane CN, Rimer IM, McAdam SAM (2022) Seeing is believing: what visualising bubbles in the xylem has revealed about plant hydraulic function. Funct Plant Biol 49:759–772.

Carlquist S (1984) Vessel grouping in dicotyledon wood: significance and relationships to imperforate tracheary elements. Aliso 10:505–525.

Charrier G, Torres-ruiz JM, Badel E et al. (2016) Evidence for hydraulic vulnerability segmentation and lack of xylem refilling under tension. Plant Physiol 172:1657–1668.

Choat B, Lahr EC, Melcher PJ, Zwieniecki MA, Holbrook NM (2005) The spatial pattern of air seeding thresholds in mature sugar maple trees. Plant Cell Environ 28:1082–1089.

Choat B, Choat B, Cobb AR, Jansen S (2008) Structure and function of bordered pits: new discoveries and impacts on whole-plant hydraulic function. New Phytol 177:608–626.

Choat B, Jansen S, Brodribb TJ et al. (2012) Global convergence in the vulnerability of forests to drought. Nature 491:752–756.

Choat B, Badel E, Burlett R, Delzon S, Cochard H, Jansen S (2016) Non-invasive measurement of vulnerability to drought-induced embolism by X-ray microtomography. Plant Physiol 170:273–282.

Choat B, Brodribb TJ, Brodersen CR, Duursma RA, López R, Medlyn BE (2018) Triggers of tree mortality under drought. Nature 558:531–539.

Cochard H, Delzon S (2013) Hydraulic failure and repair are not routine in trees. Ann For Sci 70:659–661.

Cochard H, Pimont F, Ruffault J, Martin-StPaul N (2021) SurEau: a mechanistic model of plant water relations under extreme drought. Ann For Sci 78:55.

Dória LC, Podadera DS, del Arco M, Chauvin T, Smets E, Delzon S, Lens F (2018) Insular woody daisies (*Argyranthemum*, Asteraceae) are more resistant to drought-induced hydraulic failure than their herbaceous relatives. Funct Ecol 32:1467–1478.

Flexas J, Clemente-Moreno MJ, Bota J et al. (2021) Cell wall thickness and composition are involved in photosynthetic limitation. J Exp Bot 72:3971–3986.

Gauthey A, Peters JMR, Carins-Murphy MR et al. (2020) Visual and hydraulic techniques produce similar estimates of cavitation resistance in woody species. New Phytol 228:884–897.

Guan X, Pereira L, McAdam SAM, Cao K, Jansen S (2021) No gas source, no problem: proximity to pre-existing embolism and segmentation affect embolism spreading in angiosperm xylem by gas diffusion. Plant Cell Environ 44:1329–1345.

Guan X, Werner J, Cao KF, Pereira L, Kaack L, McAdam SAM, Jansen S (2022) Stem and leaf xylem of angiosperm trees experiences minimal embolism in temperate forests during two consecutive summers with moderate drought. Plant Biol. https://doi.org/10.1111/plb.13384.

Hacke UG, Sperry JS, Pockman WT, Davis SD, Mcculloh KA (2001) Trends in wood density and structure are linked to prevention of xylem implosion by negative pressure. Oecologia 126:457–461.

Hacke UG, Spicer R, Schreiber SG, Plavcová L (2017) An ecophysiological and developmental perspective on variation in vessel diameter. Plant Cell Environ 40:831–845.

Hochberg U, Albuquerque C, Rachmilevitch S, Cochard H, David-Schwartz R, Brodersen CR, McElrone A, Windt CW (2016) Grapevine petioles are more sensitive to drought induced embolism than stems: evidence from in vivo MRI and microcomputed tomography observations of hydraulic vulnerability segmentation. Plant Cell Environ 39:1886–1894.

Hochberg U, Windt CW, Ponomarenko A, Zhang YJ, Gersony J, Rockwell FE, Holbrook NM (2017) Stomatal closure, basal leaf embolism, and shedding protect the hydraulic integrity of grape stems. Plant Physiol 174:764–775.

Hölttä T, Vesala T, Perämäki M, Nikinmaa E (2002) Relationships between embolism, stem water tension, and diameter changes. J Theor Biol 215:23–38.

Ingram S, Salmon Y, Lintunen A, Hölttä T, Vesala T, Vehkamäki H (2021) Dynamic surface tension enhances the stability of nanobubbles in xylem sap. Front Plant Sci 12:732701.

Jacobsen AL, Ewers FW, Pratt RB, Paddock WA III, Davis SD (2005) Do xylem fibers affect vessel cavitation resistance? Plant Physiol 139:546–556.

Jacobsen AL, Tobin MF, Toschi HS, Percolla MI, Pratt RB (2016) Structural determinants of increased susceptibility to dehydration-induced cavitation in post-fire resprouting chaparral shrubs. Plant Cell Environ 39:2473–2485.

Jansen S, Klepsch M, Li S, Kotowska MM, Schiele S, Zhang Y, Schenk HJ (2018) Challenges in understanding air-seeding in angiosperm xylem. Acta Hortic 1222:13–20.

Jansen S, Guan X, Kaack L, Miranda MT, Trabi C, Ribeiro RV, Pereira L (2020) The Pneumatron estimates xylem embolism resistance in angiosperms based on gas diffusion kinetics: a mini-review. Acta Hortic 1300:193–200.

Johnson KM, Brodersen C, Carins-Murphy MR, Choat B, Brodribb TJ (2020) Xylem embolism spreads by single-conduit events in three dry forest angiosperm stems. Plant Physiol 184:212–222.

Kaack L, Altaner CM, Carmesin C, et al. (2019) Function and three-dimensional structure of intervessel pit membranes in angiosperms: a review. IAWA J 40: 673–702.

Kaack L, Weber M, Isasa E et al. (2021) Pore constrictions in intervessel pit membranes provide a mechanistic explanation for xylem embolism resistance in angiosperms. New Phytol 230:1829–1843.

Kanduč M, Schneck E, Loche P, Jansen S, Schenk HJ, Netz RR (2020) Cavitation in lipid bilayers poses strict negative pressure stability limit in biological liquids. Proc Natl Acad Sci USA 117:10733–10739.

Kröber W, Zhang S, Ehmig M, Bruelheide H (2014) Linking xylem hydraulic conductivity and vulnerability to the leaf economics spectrum—a cross-species study of 39 evergreen and deciduous broadleaved subtropical tree species. PLoS One 9:e109211.

Lamarque LJ, Corso D, Torres-ruiz JM, Badel E, Brodribb TJ, Burlett R (2018) An inconvenient truth about xylem resistance to embolism in the model species for refilling *Laurus nobilis* L. Ann For Sci 88:1–15.

Larter M, Pfautsch S, Domec JC, Trueba S, Nagalingum N, Delzon S (2017) Aridity drove the evolution of extreme embolism resistance and the radiation of conifer genus *Callitris*. New Phytol 215:97–112.

Lens F, Sperry JS, Christman MA, Choat B, Rabaey D, Jansen S (2011) Testing hypotheses that link wood anatomy to cavitation resistance and hydraulic conductivity in the genus *Acer*. New Phytol 709:709–723.

Lens F, Picon-Cochard C, Delmas CEL et al. (2016) Herbaceous angiosperms are not more vulnerable to drought-induced embolism than angiosperm trees. Plant Physiol 172:661–667.

Lens F, Tixier A, Cochard H, Sperry JS, Jansen S, Herbette S (2013) Embolism resistance as a key mechanism to understand adaptive plant strategies. Curr Opin Plant Biol 16:287–292.

Levionnois S, Jansen S, Wandji RT, et al. (2021) Linking drought-induced xylem embolism resistance to wood anatomical traits in neotropical trees. New Phytol 229:1453–1466.

Li S, Lens F, Karimi Z, Klepsch MM (2016) Intervessel pit membrane thickness as a key determinant of embolism resistance in angiosperm xylem. IAWA J 37:152–171.

Li X, Blackman CJ, Choat B, Rymer PD, Medlyn BE, Tissue DT (2018) Tree hydraulic traits are coordinated and strongly linked to climate-of-origin across a rainfall gradient. Plant Cell Physiol 41:646–660.

Lima TRA, Carvalho ECD, Martins FR et al. (2018) Lignin composition is related to xylem embolism resistance and leaf life span in trees in a tropical semiarid climate. New Phytol 219:1252–1262.

Lobo A, Torres-Ruiz JM, Burlett R et al. (2018) Assessing inter- and intraspecific variability of xylem vulnerability to embolism in oaks. For Ecol Manage 424:53–61.

Loepfe L, Marinez-Vilata J, Piñol J, Mencuccini M (2007) The relevance of xylem network structure for plant hydraulic efficiency and safety. J Theor Biol 247:788–803.

Maherali H, Moura CE, Caldeira MC, Willson CJ, Jackson RB (2006) Functional coordination between leaf gas exchange and vulnerability to xylem cavitation in temperate forest trees. Plant Cell Environ 29:571–583.

Martínez-Vilalta J, Mencuccini M, Alvarez X, Camacho J, Loepfe L, Piñol J (2012) Spatial distribution and packing of xylem conduits. Am J Bot 99:1189–1196.

Mrad A, Domec J-C, Huang C-W, Lens F, Katul G (2018) A network model links wood anatomy to xylem tissue hydraulic behaviour and vulnerability to cavitation. Plant Cell Environ 41:2718–2730.

Mrad A, Johnson DM, Love DM, Domec J-C (2021) The roles of conduit redundancy and connectivity in xylem hydraulic functions. New Phytol 231:996–1007.

Olson ME, Anfodillo T, Rosell JA, Petit G, Crivellaro A, Isnard S, León-Gómez C, Alvarado-Cárdenas LO, Castorena M (2014) Universal hydraulics of the flowering plants: vessel diameter scales with stem length across angiosperm lineages, habits and climates. Ecol Lett 17:988–997.

Pereira L, Domingues-Junior AP, Jansen S, Choat B, Marrafera P (2018) Is embolism resistance in plant xylem associated with quantity and characteristics of lignin? Trees 32:349–358.

Petit G, Anfodillo T, Mencuccini M (2008) Tapering of xylem conduits and hydraulic limitations in sycamore (*Acer pseudoplatanus*) trees. New Phytol 177:653–664.

Pittermann J, Stuart SA, Dawson TE, Moreau A (2012) Cenozoic climate change shaped the evolutionary ecophysiology of the Cupressaceae conifers. Proc Natl Acad Sci USA 109:9647–9652.

Pratt RB, Castro V, Fickle JC, Jacobsen AL (2019) Embolism resistance of different aged stems of a California oak species (*Quercus douglasii*): optical and microCT methods differ from the benchtop-dehydration standard. Tree Physiol 40:5–18.

Preston KA, Cornwell WK, DeNoyer JL (2006) Wood density and vessel traits as distinct correlates of ecological strategy in 51 California coast range angiosperms. New Phytol 170:807–818.

Pritzkow C, Brown MJM, Carins-Murphy MR, Bourbia I, Mitchell PJ, Brodersen C, Choat B, Brodribb TJ (2022) Conduit position and connectivity affect the likelihood of xylem embolism during natural drought in evergreen woodland species. Ann Bot 130:431–444.

Rockwell FE, Wheeler JK, Holbrook NM (2014) Cavitation and its discontents: opportunities for resolving current controversies. Plant Physiol 164:1649–1660.

Roig-Oliver M, Douthe C, Bota J, Flexas J (2021) Cell wall thickness and composition are related to photosynthesis in Antarctic mosses. Physiol Plant 173:1914–1925.

Rosner S, Heinze B, Savi D-SG (2019) Prediction of hydraulic conductivity loss from relative water loss: new insights into water storage of tree stems and branches. Physiol Plant 165:843–854.

Sano Y, Ohta T, Jansen S (2008) The distribution and structure of pits between vessels and imperforate tracheary elements in angiosperm woods. IAWA J 29:1–15.

Sano Y, Morris H, Shimada H, Ronse De Craene LP, Jansen S (2011) Anatomical features associated with water transport in imperforate tracheary elements of vessel-bearing angiosperms. Ann Bot 107:953–964.

Schumann K, Leuschner C, Schuldt B (2019) Xylem hydraulic safety and efficiency in relation to leaf and wood traits in three temperate *Acer* species differing in habitat preferences. Trees Struct Funct 33:1475–1490.

Scoffoni C, Albuquerque C, Brodersen CR, Townes SV, John GP (2016) Leaf vein xylem conduit diameter influences susceptibility to embolism and hydraulic decline. New Phytol 213:1076–1092.

Skelton R, Diaz J (2020) Quantifying losses of plant hydraulic function: seeing the forest, the trees and the xylem. Tree Physiol 40:285–289.

Skelton RP, Dawson TE, Thompson SE, Shen Y, Weitz AP, Ackerly D (2018) Low vulnerability to xylem embolism in leaves and stems of North American oaks. Plant Physiol 177:1066–1077.

Skelton RP, Anderegg LDL, Diaz J, Kling MM, Papper P, Lamarque LJ, Delzon S, Dawson TE, Ackerly DD (2021) Evolutionary relationships between drought-related traits and climate shape large hydraulic safety margins in western North American oaks. Proc Natl Acad Sci USA 118:e2008987118.

Sorz J, Hietz P (2006) Gas diffusion through wood: Implications for oxygen supply. Trees Struct Funct 20:34–41.

Sperry JS, Pockman WT (1993) Limitation of transpiration by hydraulic conductance and xyiem cavitation in *Betula occidentalis*. Plant Cell Environ 16:279–287.

Sperry JS, Tyree MT (1988) Xylem embolism mechanism of water stress-induced. Plant Physiol 88:581–587.

Tyree MT, Cochard H (1996) Summer and winter embolism in oak: impact on water relations. Ann For Sci 52:173–180.

Vander Willigen C, Sherwin H, Pammenter N (2000) Xylem hydraulic characteristics of subtropical trees from contrasting habitats grown under identical environmental conditions. New Phytol 145:51–59.

Venturas MD, Pratt RB, Jacobsen AL, Castro V, Fickle JC, Hacke UG (2019) Direct comparison of four methods to construct xylem vulnerability curves: Differences among techniques are linked to vessel network characteristics. Plant Cell Environ 42:2422–2436.

Venturas MD, Sperry JS, Hacke UG (2017) Plant xylem hydraulics: What we understand, current research, and future challenges. J Integr Plant Biol 59:356–389.

Wang Y, Burlett R, Feng F, Tyree MT (2014) Improved precision of hydraulic conductance measurements using a Cochard rotor in two different centrifuges. J Plant Hydraulics 1:e007.

Wason J, Bouda M, Lee EF, McElrone AJ, Phillips RJ, Shackel KA, Matthews MA, Brodersen C (2021) Xylem network connectivity and embolism spread in grapevine (*Vitis vinifera* L.). Plant Physiol 186:373–387.

Wheeler JK, Sperry JS, Hacke UG, Hoang N (2005) Inter-vessel pitting and cavitation in woody Rosaceae and other vesselled plants: a basis for a safety versus efficiency trade-off in xylem transport. Plant Cell Environ 28:800–812.

Yang D, Pereira L, Peng G, Ribeiro RV, Kaack L, Jansen S, Tyree MT (2022) A Unit Pipe Pneumatic model to simulate gas kinetics during measurements of embolism in excised angiosperm xylem. Tree Physiol. https://doi.org/10.1093/treephys/tpac105.

Zanne AE, Westoby M, Falster DS, Ackerly DD, Loarie SR, Arnold SEJ, Coomes DA (2010) Angiosperm wood structure: global patterns in vessel anatomy and their relation to wood density and potential conductivity. Am J Bot 97:207–215.

Zhang J, Yu G, Wen W, Ma X, Xu B, Huang B (2016) Functional characterization and hormonal regulation of the PHEOPHYTINASE gene LpPPH controlling leaf senescence in perennial ryegrass. J Exp Bot 67:935–945.

Zhang Y, Rockwell FE, Graham AC, Alexander T, Holbrook NM (2016) Reversible leaf xylem collapse: a potential "circuit breaker" against cavitation. Plant Physiol 172:2261–2274.

Zhang Y, Carmesin C, Kaack L et al. (2019) High porosity with tiny pore constrictions and unbending pathways characterise the 3D structure of intervessel pit membranes in angiosperm xylem. Plant Cell Environ 43:116–130.

Zimmermann M, Tomlinson P (1966) Analysis of complex vascular systems in plants: optical shuttle method. Science 152: 72–73.